INITIATIVE ON
Digital Innovation

TECHNICAL REPORT

Mapping of Rice Areas in Egypt using SAR Imagery

Renaud Mathieu ✉
International Rice Research Institute (IRRI)

Abstract Egypt is the second biggest rice producer in Africa after Nigeria and produces rice mostly during the summer season. Annual estimations of crop areas and yield are derived using information collected on the ground by extension services and released by the Ministry of Agriculture. However, sample sizes are usually small and can not be easily expanded due to costs and staff shortages. In addition, crop area and production estimates are released after harvest, which is too late to be used for interventions. Timely, accurate, and actionable information on rice areas and production is essential for improving food security policy decisions. This use case aims to develop a digital rice monitoring platform in Egypt based on near-real-time satellite data to support national policies, food security, and market management, as well as to facilitate farmers' resilience through the development of insurance and microfinance products. This report presents the preliminary results of mapping rice areas across the Nile Delta during the 2022 summer season using IRRI's RIICE platform in collaboration with Tanta University and European Space Agency.

Date: **13 Dec 2022** // Work Package: **4. Real-time Monitoring** // Partners: **IRRI, Tanta Univ., ESA**

Table of Contents

Mapping of Rice Areas in Nile Delta, Egypt, using SAR Imagery

Abstract

Egypt is the second biggest rice producer in Africa after Nigeria and produces rice mostly during the summer season. Annual estimations of crop areas and yield are derived using information collected on the ground by extension services and released by the Ministry of Agriculture. However, sample sizes are usually small and can not be easily expanded due to costs and staff shortages. In addition, crop area and production estimates are released after harvest, which is too late to be used for interventions. Timely, accurate, and actionable information on rice areas and production is essential for improving food security policy decisions. This use case aims to develop a digital rice monitoring platform in Egypt based on near-real-time satellite data to support national policies, food security, and market management, as well as to facilitate farmers' resilience through the development of insurance and microfinance products. This report presents the preliminary results of mapping rice areas across the Nile Delta during the 2022 summer season using IRRI's RIICE platform in collaboration with Tanta University and European Space Agency.

1. Introduction

Rice is one of the most important crops in Egypt, with an average production estimated at 4.6 million metric tons in the 2019-2021 summer seasons and a harvested area of about 1.2 million feddans (500K ha; MALR, 2019; 2020; 2021). The country is characterized by hot, dry summers from May to October and mild winters from November to April. The total population in 2019 was estimated at 100.4 million, 58% of which are rural (FAO, 2022). About 95% of the total population lives in the Nile Valley and Delta (MWRI, 2005). Egypt's gross domestic product (GDP) in 2019 was estimated at US$ 317 billion, of which the agriculture sector accounted for 11.05% or around US$ 35 billion (FAO, 2022). Agriculture remains a major economic activity in the country.

Egypt is the second biggest rice producer in Africa after Nigeria and produces rice mostly during the summer season, which contributes 97% of the total national rice production. A national workshop is planned in Egypt in early 2023 to engage Egyptian authorities (Ministries, NARES) and stakeholders and define an implementation roadmap.

Tolba et al. (2020) mapped rice areas over parts of the Nile Delta using the Normalized Difference Vegetation Index (NDVI) and Land Surface Temperature (LST). They were able to differentiate rice from other crops that have similar life cycles to rice at the early development stages due to low NDVI values of rice caused by the typical agronomic flooding. Using LST, rice was differentiated from other crops in all of the development stages, from flooding to harvest. The use of Synthetic Aperture Radar (SAR) imagery has been proven effective in accurately mapping and monitoring rice areas based on the temporal variability of microwave-plant-water interactions (Ribbes and Le Toan, 1999; Rosenqvist, 1999), especially

during the Monsoon or rainy season when clouds are prevalent (Nelson et al. 2014, Bouvet et al. 2009, Le Toan et al. 1997). Several studies on the use of SAR in mapping rice and detecting its phenological stages have been tested in various countries such as Vietnam (Chen et al. 2016, Nguyen et al. 2016, Lasko et al. 2017), China (Mansaray et al. 2017), Myanmar (Torbick et al. 2017), France (Bazzi et al. 2019), Taiwan (Nguyen et al. 2021), and the Philippines (Mabalay et al. 2022).

The methodology used in this study builds on geospatial technology developed since 2011 through the Remote Sensing-based Information and Insurance for Crops in Emerging Economies (RIICE, http://www.riice.org/). It intends to answer the following questions: where is rice, when is rice, and how much will be/is rice yield? The service was developed and implemented by sarmap and IRRI, institutionally supported and co-founded by the Swiss Development Cooperation, and the initial years focused on development in South-East and South Asia. RIICE relies on the integration of Synthetic Aperture Radar derived products – rice area, the beginning of the rice crop season, Leaf Area Index (LAI) – and a crop growth simulation model – ORYZA – to provide spatially explicit forecasts and estimate yield at harvest time. Given the spatial and temporal information provided by remote sensing data, the model is scalable to any extent – with the use of local rice agronomic knowledge incorporated in a rice ecosystem model – and it makes it possible to attain detailed spatial yield information at 1-2 ha. After a successful two-year pilot across 13 sites covering 4.8 million ha in Asia, RIICE has been upgraded to an operational rice monitoring system. The launch of ESA's Sentinel-1 satellite ensured the continued availability of SAR data at no cost. Today, the system is operationally used in the Philippines (https://prism.philrice.gov.ph/), Cambodia, Vietnam, and three Indian states: Odisha, Andhra Pradesh, and Tamil Nadu. As part of the CGIAR Research Initiative on Digital Innovation, IRRI aims to adapt, calibrate, and develop the RIICE

technology for Egypt in collaboration with Tanta University and local government and NARES partners.

This report covers the initial rice area and the start of season maps and estimates produced over the Nile Delta for the 2022 Summer Season.

2. Data and Methods

2.1. Study area

Egypt rice cultivation is concentrated in the Delta primarily because of its soils which are composed of a thick clay layer, the formation of which is associated with the deposition of sediments that are continuously carried along the Nile course through floods. Soil drainage is consequently hampered by heavy clays and favor flooded crops such as paddy (Ahmed, 1998). The northern strip of the Delta is characterized by highly saline groundwater due to subsurface intrusion of seawater and/or marine ingress attributed to continuous submergence of this part of the Delta under seawater in historical periods (Hefny et al. 1995). Rice cultivation is usually rotated with cotton and maize cultivation in the two types of crop rotation commonly carried out in the Nile Delta (i.e., two-year and three-year rotation systems)(Ahmed, 1998). Those rotation systems present two patterns of crop rotation in Egypt. One of them includes rice with the rotation (i.e., berseem, wheat, rice, cotton, maize, and beans) and other without rice (i.e., berseem, cotton, wheat, maize, beans, and vegetables)(El-Shahway et al. 2016).

The study area covers the six production zones of the Nile Delta, including the governorates of Damietta, El Dakahlia, Kafr el Sheikh, El Sharkia, El Beheira, and El Gharbia. Rice is cultivated during the summer season. These governorates constitute 97% of the total rice harvested area in the Delta. Among these

governorates, Dakahlia was ranked first both in terms of production and area harvested.

2.2. Data

Satellite data

Multi-temporal C-band Synthetic Aperture Radar (SAR) imagery, specifically Sentinel-1A (S-1A), was obtained freely from the Copernicus Open Access Hub (https://scihub.copernicus.eu). A total of 51 S-1A images were acquired from 06 April to 09 November 2022, both from ascending and descending orbits were used to delineate rice areas and identify the start of season (SOS) dates. The acquisition dates cover the rice growing season from flooding, sowing, and planting up to harvest.

Other data used include the 30m Digital Elevation Model (DEM) from Shuttle Radar Topography Mission (SRTM) and optical imagery such as Landsat 8-9. A total of 48 Landsat images from 5 April to 15 November 2022 were obtained from USGS earth explorer. NDVI images derived from Landsat 8-9 were used as input to create the rice-nonrice mask and in rice classification. DEM was used as input in image pre-processing and classification.

Table 1 shows the characteristics of the satellite data used in rice mapping, and Figure 1 shows the study area and the footprints of the SAR data. The study area is fully covered by the combined footprints.

Table 1 Characteristics of satellite data used in mapping rice and the start of the season.

Satellite, Band	**Sentinel-1A (SAR-C)**			**Landsat 8-9**	
Sensor type	Radar			Optical	
Mode	Interferometric Wide swath (IW)			-	
Product type	Ground Range Detected (GRD)			Level 1	
Swath width (km)	200x250			185x180	
Resolution	20 m			30 m	
Polarization, incidence angle	VV VH, 40° at scene center			-	
Repeat cycle (days)	12			16	
Relative orbit (S-1A); Path/Row (Landsat 8-9)	58	167	65	177/038 177/039	176/038 176/039
Pass direction	Ascend	Descend		Descend	
No of frames	2	2	1	2	2
Acquisition dates (2022)					
Start date	06-Apr	26-Apr	07-Apr	15-May	08-May
End date	08-Nov	04-Nov	09-Nov	15-Nov	08-Nov
# missing acquisitions	3	1			
# acquisitions	16	16	19	24	24

Secondary data

Official statistics on rice areas for the last four years (e.i., 2018-2021) were obtained from published data by the Ministry of Agriculture and Land Reclamation (MALR) (Figure 2). Rice harvested area map at the global level (SPAM 2010 v2.0) was obtained from International Food Policy Research Institute (IFPRI, 2019). These data were used to assess the trend in rice harvested area over the years (official

statistics) and to compare the initial estimates of rice area based on SAR (official statistics and SPAM).

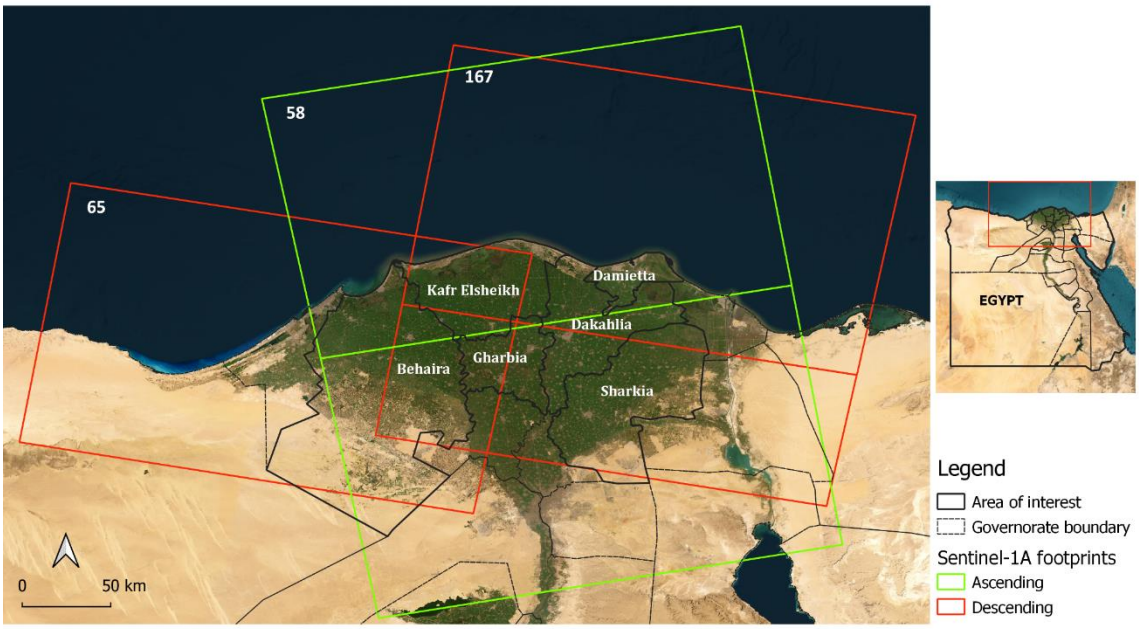

Figure 1 Sentinel-1A footprints over the Nile Delta. Governorate names are shown only for the area of interest (AOI). Numbers refer to the relative orbit number used in Table 1. The right map shows the location of the AOI in Egypt.

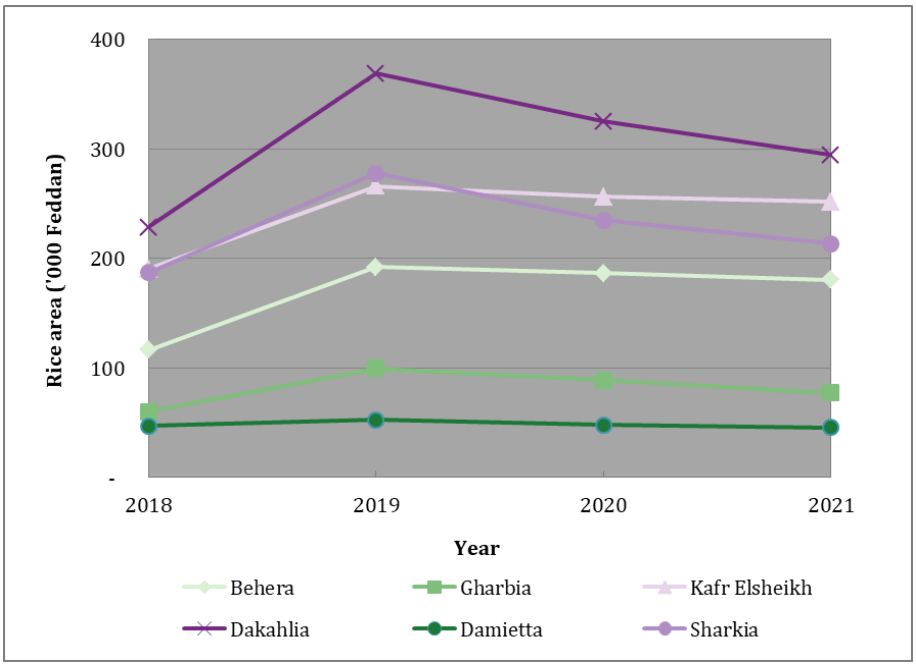

Figure 2 Rice harvested area in the AOI from 2018-2021 Summer Season reported by MALR.

2.3 Methods

A combination of Sentinel-1A and Landsat 8-9 imagery was used to detect and map cultivated rice areas and the start of the season. The algorithm analyzed in parallel the SAR multitemporal acquisition series (i.e., ascending and descending passes and co (VV) and cross (VH) polarizations) and NDVI derived from Landsat 8-9 images. The rice temporal signature and the start of the season are first detected from the SAR series, then cross-checked with the NDVI values using predefined rules. The overview of the methodology used in this study is presented in Figure 3. Each step is discussed in detail in the following subsections.

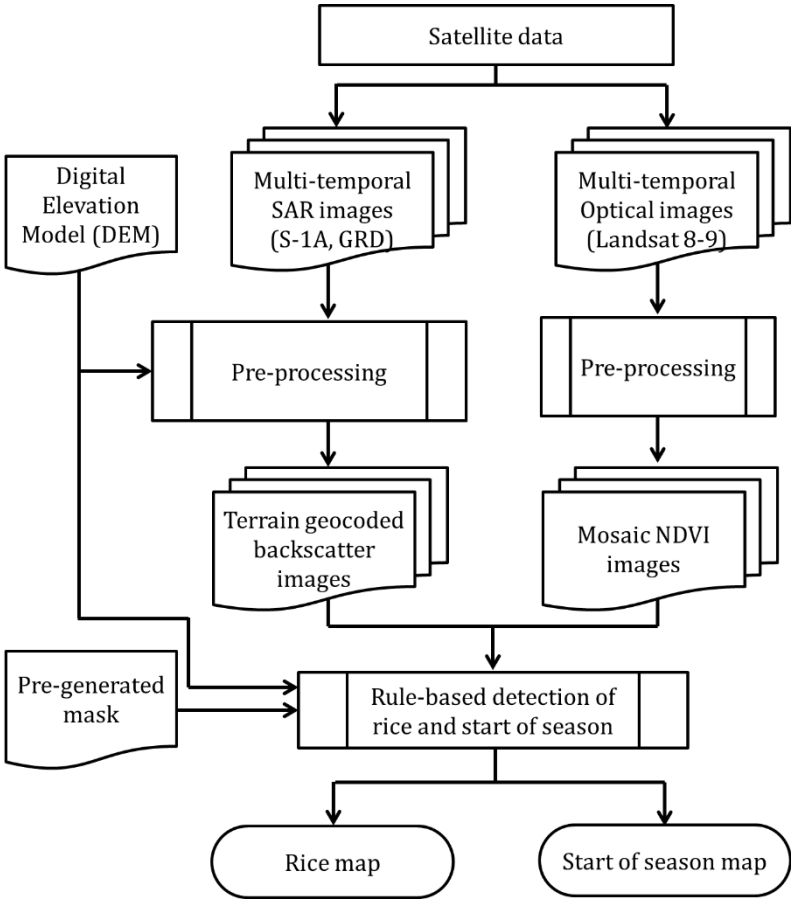

Figure 3 Flowchart of the method applied in the study.

Pre-processing of satellite images

MAPscape-RICE, an image processing software developed by sarmap specifically for rice information extraction, was used to process the satellite images and to classify rice. The pre-processing step, which was fully automated, sequentially performed a series of steps to convert the multi-temporal SAR GRD data into terrain geocoded backscatter δo values. The pre-processing, described in detail in Holecz et. al, 2013 and Nelson et al. 2014, include the following steps: (1) strip mosaicking - this step mosaicked single frames of the same orbit and acquisition dates along the azimuth and generated a strip in slant range geometry; (2) coregistration - images acquired with the same observation geometry and mode were coregistered in slant range geometry; (3) time series speckle filtering - an optimum weighting filter was applied to balance differences in reflectivity between images at different times within the multi-temporal filtering; (4) terrain geocoding, radiometric calibration and normalization - Digital Elevation Model (DEM) was used to convert the position of the δo elements into slant range image coordinates; (5) anisotropic non-linear diffusion (ANLD) filtering - this filter smoothes homogenous targets and enhances the differences between neighboring areas; and (6) removal of atmospheric attenuation - although microwave signals have the ability to penetrate clouds, it is possible that δo from a shorter wavelength (e.g. C-band) can be locally attenuated by water vapor due to tropical storms. In this step, anomalous high backscatter peaks or troughs were adjusted or corrected using an interpolator.

Mask generation

A mask was generated using multi-temporal features extracted from Landsat 8-9's NDVI images and from Sentinel-1A VH polarization intensity images. The mask was used to discard pixels that were certainly not rice.

Rice and start of season detection

The multi-temporal stack of terrain geocoded δo images was analyzed to set different thresholds using a rule-based detection algorithm. Rice areas were detected from the SAR temporal signature following these steps: rice exclusion, detection of agronomic flooding, and evidence of rice growth, and the last rule looks at a drop in backscatter.

For the rice exclusion step, conditions were applied to the temporal signature for each pixel to mask out: (1) areas with consistently low backscatter values, typical for stable water bodies; (2) areas with consistently high backscatter values, typical for built-up areas or infrastructures; (3) areas where the backscatter remain below the minimum value longer than the maximum time underwater, i.e., flooding longer than agronomic flooding for rice, but not permanent floodings, such as in fishponds or wetlands; and (4) areas with unusually high variation in backscatter. Rice shows variation in backscatter values over time, but there is a maximum variation that can be expected in biomass. Any pixel that satisfied one or more of these exclusion conditions was labeled non-rice and excluded from further analysis. Consequently, any pixel that does not satisfy any of these criteria was retained for further analysis. Using the temporal series (i.e., from the first to the last image), the second rule looked at any evidence of agronomic flooding at the start of the season. Flooded rice fields exhibit low backscatter values at SoS. Once the flooded condition was detected, the next rule looked at evidence of crop growth based on: (1) an observed increase in backscatter between SoS to minimum δo value at maximum peak and (2) the variation in the δo signature reached a minimum that is consistent with what is observed for rice crop. Pixels that meet these conditions were retained for further processing as potential rice pixels. The final rule looked for any unexpected

drops in backscatter that would indicate either a flood or a new cropping season. If this condition was satisfied, the pixel was labeled as rice.

Likewise, rules were applied to detect the possible start of season dates using VV and VH polarizations and NDVI images. This method was tested by Raviz et al. (2018) in the Philippines. The parameters used for detecting potential SoS dates include the maximum and minimum backscatter values at SoS. The maximum δo value was used to identify possible rice pixels; if the backscatter is lower than the threshold in the certain acquisition, the pixel represents a potential SoS date. The minimum δo value was used to discard possible non-rice pixels; if the backscatter is lower than the threshold in the certain acquisition, the pixel cannot correspond to an SoS date. Pixels that meet these conditions were retained for the identification of potential SoS dates. The SoS dates were assigned based on the weights used to compute the reliability coefficient (RC). For each potential SoS date, the parameters used in the computation of RC include (1) backscatter value detected as SoS from SAR input (ascending and descending, VV and VH polarizations); (2) trend of the SAR temporal signature, showing backscatter increase from SoS; (3) correspondence of SAR date from the SAR inputs; (4) consistency of backscatter with NDVI value; and (5) value of the local incidence angle (LIA) in areas covered by more than one relative orbit. Higher RC was assigned to the relative orbit with a large viewing angle. These parameters were considered on the basis of their own weight factor. The RC is obtained by summing up the contribution of each input multiplied by its own weight factor. The SoS date was assigned to the pixel with the highest RC.

3. Preliminary results

3.1. Rice area map

Rice exhibits a unique backscatter signature. Hence general rules can be applied to detect rice. However, rice is grown in a range of environmental and management conditions that vary across places and seasons. The temporal rice signature depends on agroecological zones, crop practices, and crop calendars, among others. To correctly identify rice, it is important to have prior agronomic knowledge of the area of interest, and in addition, field data and observations are crucial in setting and adjusting the mapping thresholds. These were not available in the current exercise.

The preliminary map and area estimates by governorates are shown in Figure 4 and Table 2, respectively. A total of 1.5 million feddans (653 thousand ha) were planted for rice. Of these, 24% (153 thousand ha) was detected in Sharkia (top 1), followed by Dakahlia (top 2) at 22%, as opposed to the official statistics in 2021, where the harvested area in Dakahlia was 28% (top 1) and 20% in Sharkia (top 3).

Some circular farm patterns (south of El Beheira) were detected as rice because the signature resembles that of rice (Figure 5). These crop circles are a result of center pivot irrigation and are usually planted with potatoes, wheat, or medicinal and aromatic plants such as chamomile. The maturity of spring wheat is 120 days, and potato is between 80-100 days (same as rice). These areas will be validated with partners if, indeed, these fields are planted with rice or were misclassified. Calibration field data are usually used when RIICE is used in new geographies and will be used in the future.

The likely high commission error may be due to the misclassification of “crop circles” as rice (if indeed these are not rice) and possibly other crops. Compared

with the government's statistics on the area and production of rice released in 2019-2021, the total estimate of rice area covered in the AOI based on these preliminary maps was overestimated by around 30% (Table 2). This can be addressed by adjusting the thresholds used in the rule-based classifier based on field data and local knowledge of the operators. In this part, information on crop management practices, maturity duration, crop calendar, and cropping systems from field observation are crucial.

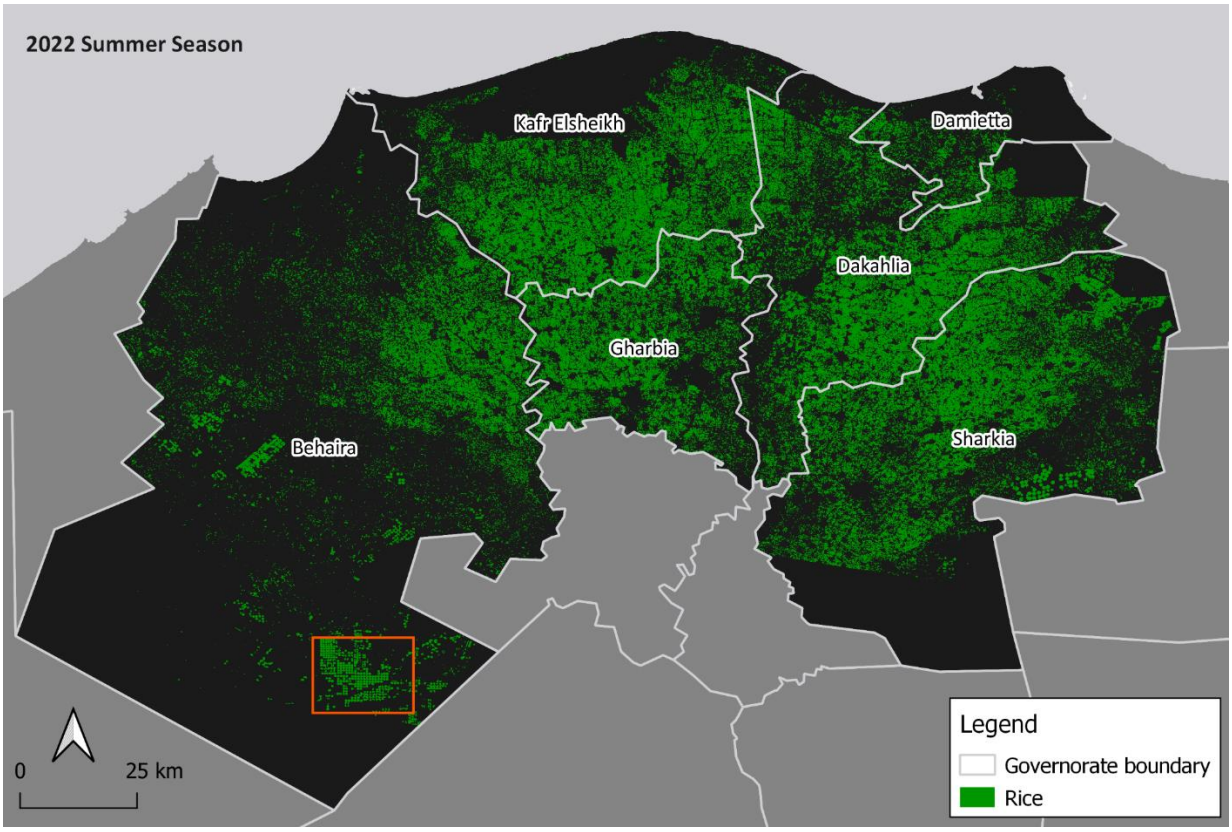

Figure 4 Rice area map generated over parts of Nile Delta, 2022 Summer Season. The red box in South Beheira covers the area with crop circles that were detected as rice.

Table 2 Comparison of area estimates between the SAR-based rice map and official statistics (survey-based) by governorate. The positive percent difference indicates that the SAR-based estimates are overestimated.

Governorate	SAR-based		Official statistics		Percent difference	
	2022 Summer season		2021	Average 2019-21	2021	Average 2019-21
	Hectare	Feddan	Feddan		(%)	
Dakahlia	141,473	336,840	294,513	329,507	13	2
Behaira	125,370	298,500	180,648	186,482	49	46
Gharbia	84,032	200,077	77,217	88,589	89	77
Sharkia	153,407	365,254	213,487	242,107	52	41
Damietta	14,408	34,306	46,000	48,875	-29	-35
Kafr Elsheik	133,859	318,712	251,857	257,962	23	21
Total	**652,550**	**1,553,689**	**1,063,722**	**1,153,523**	**37**	**30**

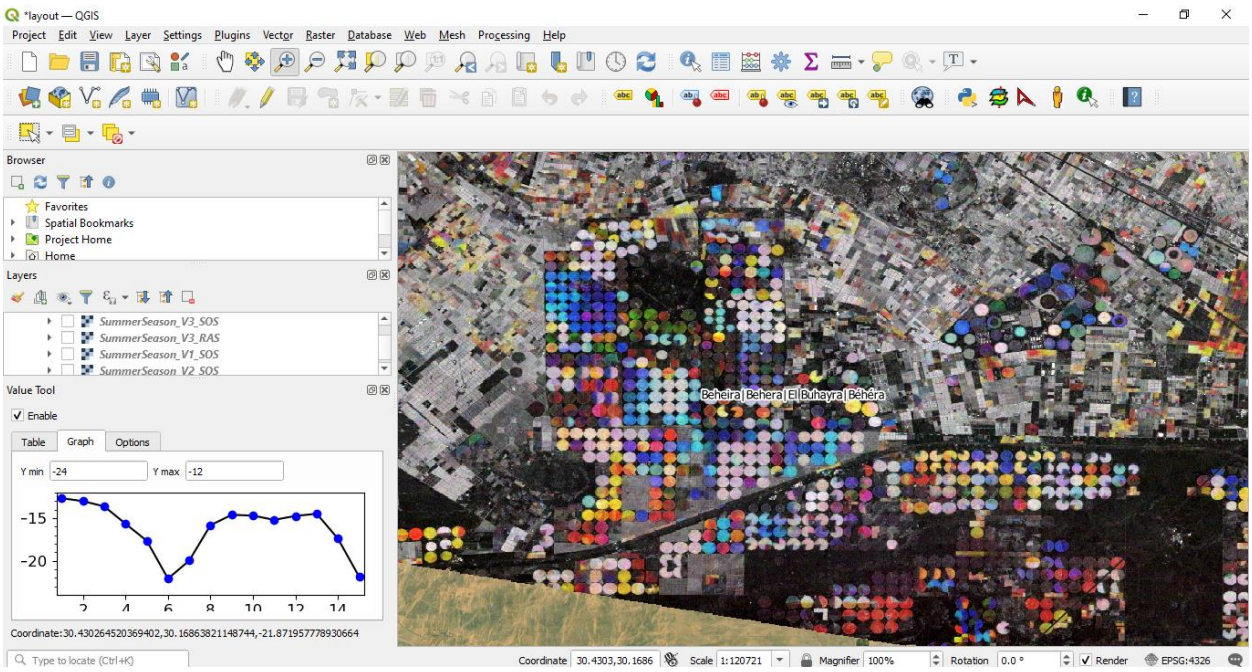

Figure 5 Screenshot of crop circles in South El Beheira, the area in the red box in Figure 3. The graph in the lower left shows a sample temporal signature of one of the crop circles.

The preliminary results were also compared with the available spatial datasets on rice by Tolba et al. (2019), IFPRI (2019), and Yu et al. (2020). Tolba et al. (2020) used NDVI and LST derived from Landsat-8 imagery acquired between May to August 2016 to delineate paddy areas. The methodology was based on the analysis of the temporal NDVI profile, where there was a rapid increase in NDVI value after the agronomic flooding period, where NDVI values were usually low. In terms of LST analysis, in rice fields, when the soil was bare, the LST value was high, and then it decreased when fields were flooded. After transplanting, with rice growth, the LST value rapidly decreased and increased again after harvest. This feature differentiates rice from other crops.

The global gridded agricultural production maps produced by IFPRI (2019) and published by Yu et al. (2020) are an improvement of the Spatial Production Allocation Model 2000 (SPAM 2000). SPAM 2010, the latest global spatial datasets on agricultural production, include estimates of crop area, yield, and production of 42 major crops at national and subnational levels.

The comparison in area estimates (Table 3) and the difference between the datasets (Figure 6) showed that the total preliminary estimates based on SAR were higher than the other two datasets, i.e., 11% and 27%, higher than the Landsat-8 and SPAM 2010 estimates, respectively. In Dakahlia and Damietta governorates, the SAR-based rice area estimates were lower by about 20% and 53% compared to the Landsat-based estimates and 15% and 39% compared to the SPAM data, respectively. The SAR-based estimates were higher than the other two datasets in the rest four governorates. The differences in the estimates could be attributed to the time of observations, data and methods used, actual changes in the ground, and other factors. In all of these three spatial datasets, the total estimates were higher compared to the official statistics estimated by MALR.

Table 3 Comparison of rice area estimates derived from SAR and other spatial datasets by governorate.

Governorate	SAR-based, 2022		Landsat-based, 2016*		SPAM, 2010**	
	Hectare	Feddan	Hectare	Feddan	Hectare	Feddan
Dakahlia	141,473	336,840	173,057	412,041	164,332	391,267
Behaira	125,370	298,500	80,980	192,811	68,309	162,640
Gharbia	84,032	200,077	59,132	140,791	62,638	149,139
Sharkia	153,407	365,254	128,229	305,307	92,423	220,053
Damietta	14,408	34,306	24,689	58,785	21,347	50,827
Kafr Elsheik	133,859	318,712	120,837	287,708	90,535	215,559
Total	652,550	1,553,689	586,926	1,397,442	499,584	1,189,485

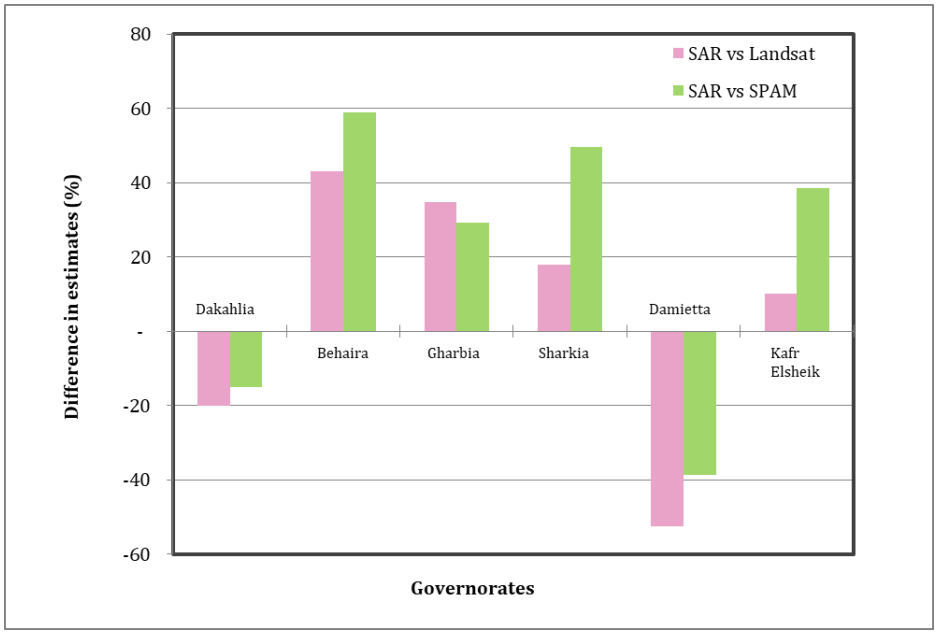

Figure 6 Difference (in percent, %) between the preliminary results derived from SAR and the Landsat-based and SPAM estimates, respectively. The negative value indicates the preliminary result was lower, while the positive value indicates the preliminary result was higher.

3.2. Start of season map

The start of the season was detected from April to August (Figure 7). Across the governorate, the majority of planting was observed in June, i.e., 59-80%, followed by planting in May, around 15-35% of the planted area (Table 4). Based on the total area planted, around 63% (413 thousand ha; 983 thousand feddans) were planted in June. These preliminary results will be validated with partners to check if the start of seasons was mapped correctly or if there were some false detections. If there were false detections, temporal signatures would need to be further investigated.

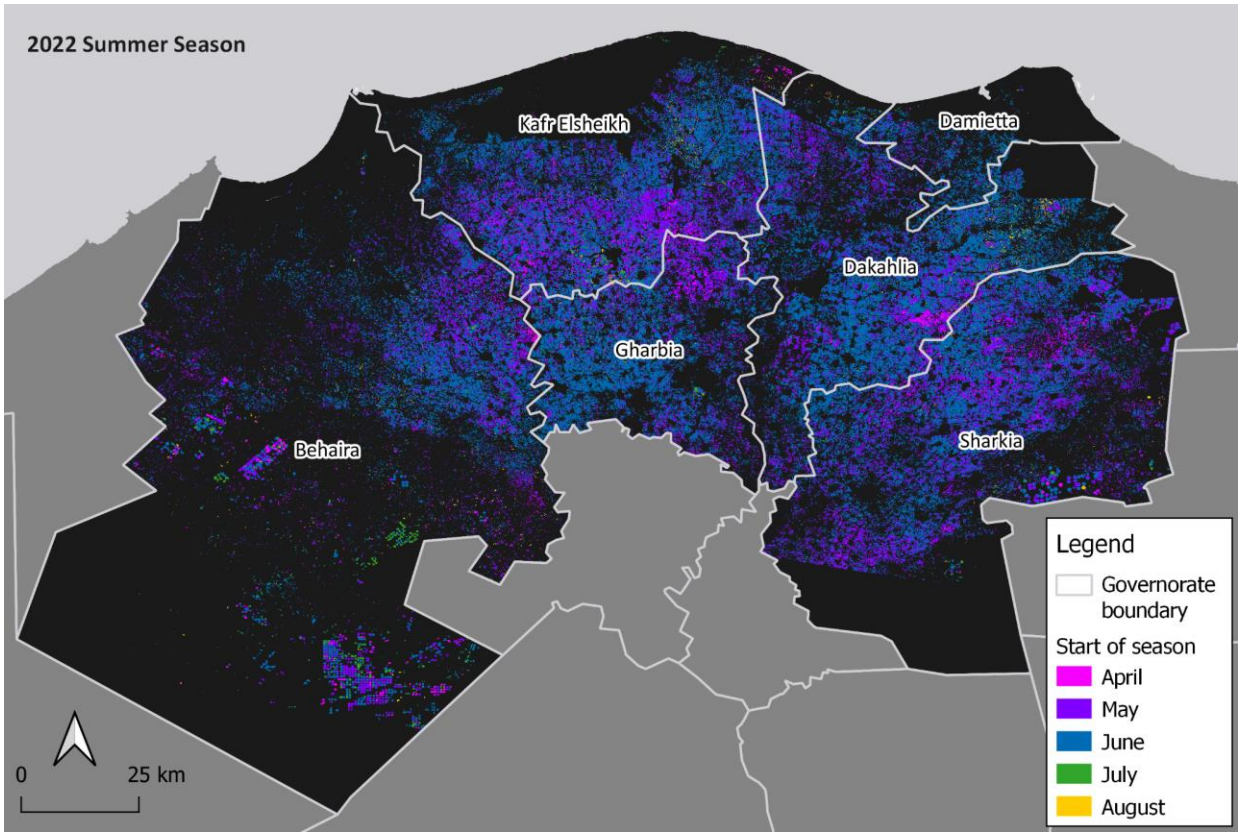

Figure 7 Start of season map derived from SAR over parts of Nile Delta, 2022 Summer Season.

Table 4 Rice area estimates in the AOI by month of planting and by governorate, 2022 Summer season.

Governorate	Rice area planted (Feddan) by month				
	April	**May**	**June**	**July**	**August**
Dakahlia	10,231	78,975	239,319	3,344	4,970
Behaira	20,914	89,599	169,839	13,448	4,701
Gharbia	10,265	47,754	138,633	1,982	1,443
Sharkia	18,646	126,399	214,425	3,408	2,377
Damietta	724	5,003	27,519	692	369
Kafr Elsheik	17,475	98,278	193,250	3,497	6,212

3.3. Rice maps and area estimates at the subdivision level

Among the governorates, the highest overestimation in rice area was observed in Gharbia (Table 2). To further assess this result, the area by subdivision was likewise estimated. The distribution of rice and the start of the season by a month in Gharbia, where Tanta University is located, are shown in Figure 8 and Figure 9, respectively. The majority of planting in Gharbia occurred in June, around 69% of the total area planted. Tanta was the second highest subdivision planted to rice (37,000 feds), next to Al-Mahallah-Kubra (46,000 feds) (Table 5). The same pattern was observed in Tanta, where the majority of planting was observed in June, around 86% (32,000 feds).

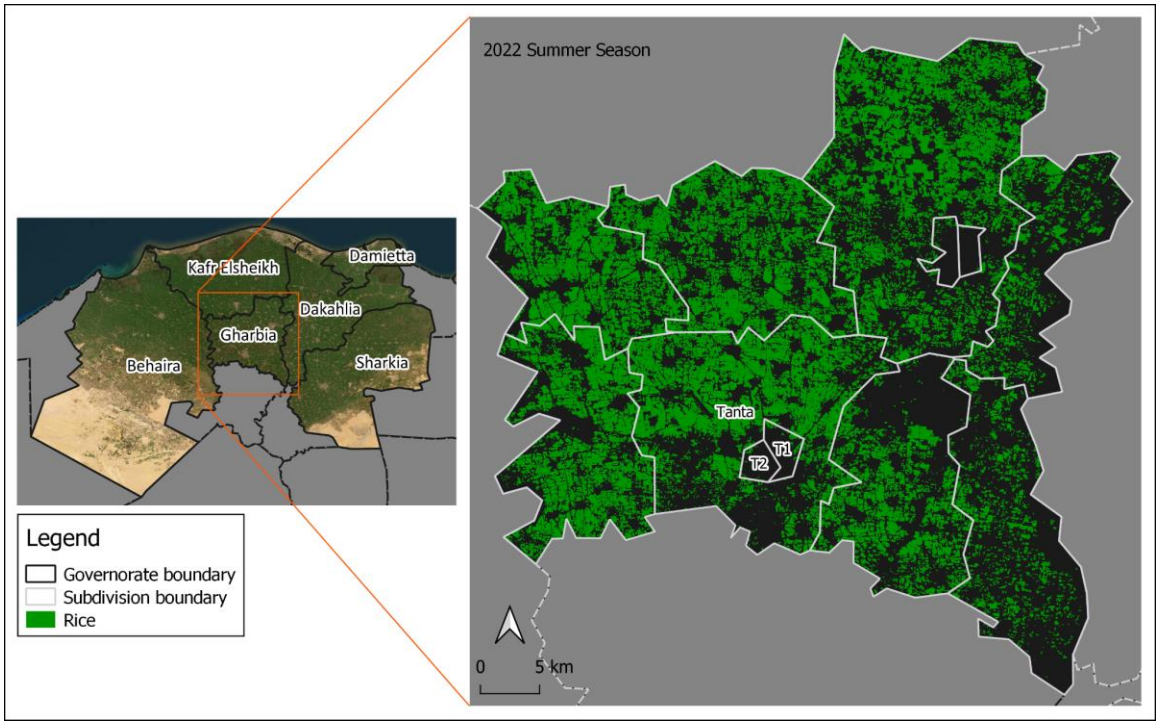

Figure 8 Rice area map in Gharbia, 2022 Summer season. The inset map shows the location of Gharbia among the AOIs.

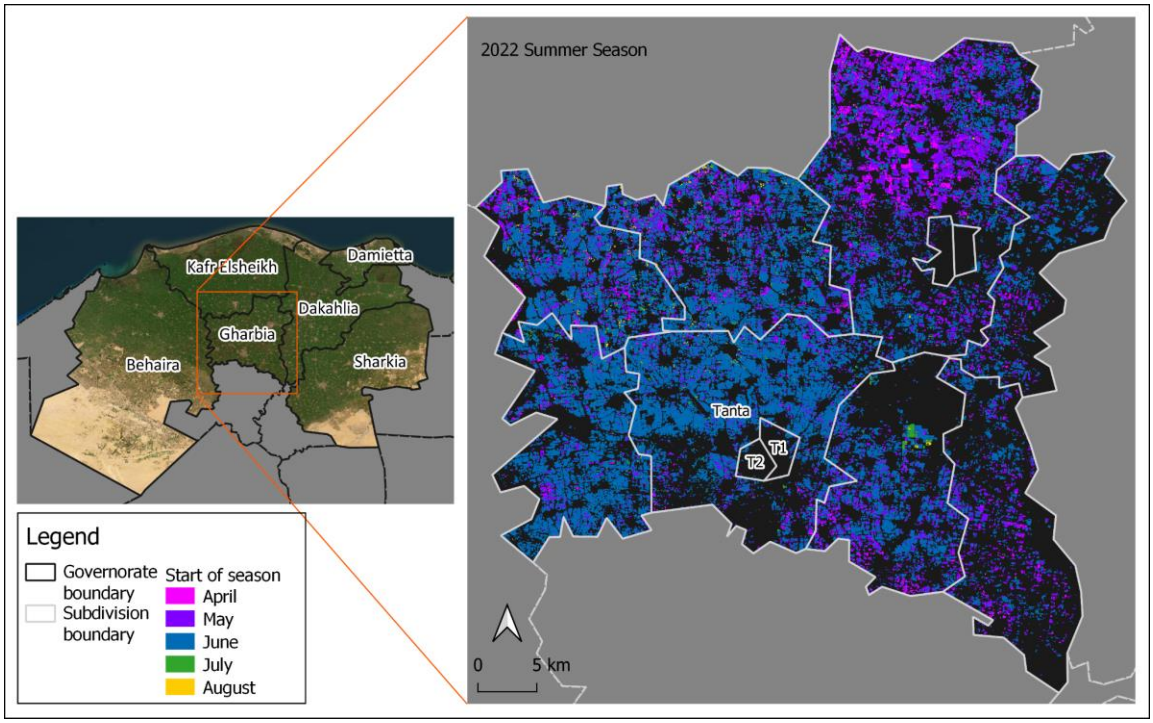

Figure 9 Start of season map in Gharbia, 2022 Summer season. The inset map shows the location of Gharbia among the AOIs.

Table 5 Estimates of rice and planting by month in Gharbia, by subdivision, 2022 Summer season.

Subdivision	Rice area (Feddan)	Rice area (Feddan) planted by month				
		April	May	June	July	Aug
Al-Mahallah al-Kubra	45,719	4,607	20,605	20,047	241	218
Al-Mahallah al-Kubra 1	60	-	4	56	0	0
Al-Mahallah al-Kubra 2	279	9	77	189	0	4
As-Santah	17,702	737	4,697	11,846	371	52
Basyun	23,661	1,159	3,883	17,871	299	449
Kafr az-Zayyat	25,823	410	2,391	22,675	285	62
Qutur	30,460	1,663	5,694	22,218	388	497
Samannud	9,219	337	2,632	6,208	29	12
Tanta	36,953	613	4,018	31,848	330	145
Tanta 1	334	0	61	272	1	-
Tanta 2	151	1	19	128	3	-
Zifta	9,702	728	3,669	5,270	32	4

4. Concluding Remarks

This rice mapping exercise was carried out by IRRI as an initial step and as a first demonstration of RIICE in the local context for our collaborators and partners in Egypt. The mapping was done without any support of field data, which are required to calibrate and validate the system and assess the accuracy of the products, especially when moving into a new geographical area or rice agronomic context.

Rice and non-rice field samples are normally used to train the remote sensing classifier and assess its performance via quantitative indicators. These could not yet

be made available in 2022. In addition, very limited knowledge was available to our analysts in terms of local rice production and agronomic practices, which are essential to fine-tune the rice area and the start of the season detection.

We expect that the maps should represent the general local rice production context, but they would need to be formally assessed by local experts and surely improved using local information. It is expected that a full-scale pilot mapping exercise, including yield estimation, will be done for the 2023 Summer season. Data are also currently collected for facilitating the generation of seasonal yield information using the integration of remote sensing data and the ORYZA rice process-based models. These datasets include weather, soil, and agronomic practices such as irrigation, fertilizer, etc.

5. References

Ahmed, TA., 1998. Worth of rice cultivation in the Nile delta. In: 24th WEDC conference, Sanitation and water for all. Islamabad, Pakistan.

Bazzi, H., Baghdadi, N., El Hajj, M., Zribi, M., Minh, D.H.T., Ndikumana, E., Courault, D., Belhouchette, H. 2019. Mapping Paddy Rice Using Sentinel-1 SAR Time Series in Camargue, France. Remote Sens. 2019, 11, 887. https://doi.org/10.3390/rs11070887

Bouvet, A., Le Toan, T., Lam-Dao, N., 2009. Monitoring of the rice cropping system in the Mekong delta using ENVISAT/ASAR dual polarization data. IEEE Transactions in Geoscience and Remote Sensing, 47, pp. 517–526.

Chen, C., Son, N., Chen, C., Chang, L., Chiang, S. 2016. Rice crop mapping using Sentinel-1A phenological metrics. International Archives of the Photogrammetry, Remote Sensing and Spatial Information Sciences. 41, p. B8.

El-Shahway, AS., Mahmoud, MMA, Udeigwe, TK. 2016. Alterations in soil chemical properties induced by continuous rice cultivation: a study on the arid Nile delta soils of Egypt. Land Degrad Dev 27:231–238.

FAO. 2022. AQUASTAT Database. http://www.fao.org/aquastat/statistics/query/index.html. Date accessed: 18 November, 2022.

Hefny, K., and Shata, A., 1995. Strategies for Planning and Management of Groundwater in the Nile Valley and Delta in Egypt, SRP Working Paper Series No. 31-1, MPWWR, Cairo.

Holecz, F., Barbieri, M., Collivignarelli, F., Gatti, L., Nelson, A., Setiyono, T.D., Boschetti, M., Manfron, G., Brivio, P.A., Quilang, E.J., et al. 2013. An operational remote sensing-based service for rice production estimation at national scale. In: Proceedings of the Living Planet Symposium 2013, Edinburgh, UK, 9-11 September 2013; ESA: Edinburgh, UK.

International Food Policy Research Institute. 2019. "Global Spatially-Disaggregated Crop Production Statistics Data for 2010 Version 2.0", https://doi.org/10.7910/DVN/PRFF8V, Harvard Dataverse, V4

Lasko, K., Vadrevu, K. P., Tran, V. T., and Justice, C. 2017. Mapping Double and Single Crop Paddy Rice With Sentinel-1A at Varying Spatial Scales and Polarizations in Hanoi, Vietnam. IEEE Journal of Selected Topics in Applied Earth Observations and Remote Sensing.

Le Toan, T., Ribbes, F., Wang, L.F., Floury, N., Ding, K.H., Kong, J.A., Fujita, M., Kurosu, T., 1997. Rice crop mapping and monitoring using ERS-1 data based on experiment and modeling results. IEEE Transactions In Geoscience and Remote Sensing, 35, pp. 41–56.

MALR. 2019. The Agricultural Statistics Bulletin, Part 2 Summer and Nili Crops 2019. Economics Affairs Sector, Ministry of Agriculture and Land Reclamation, Arab Republic of Egypt. Published data. Accessed 18 November, 2022.

MALR. 2020. The Agricultural Statistics Bulletin, Part 2 Summer and Nili Crops 2020. Economics Affairs Sector, Ministry of Agriculture and Land Reclamation, Arab Republic of Egypt. Published data. Accessed 18 November, 2022.

MALR. 2021. The Agricultural Statistics Bulletin, Part 2 Summer and Nili Crops 2021. Economics Affairs Sector, Ministry of Agriculture and Land Reclamation, Arab Republic of Egypt. Published data. Accessed 18 November, 2022.

Mabalay, M.R., Raviz, J., Alosnos, E., Barbieri, M., Quicho, E., et al. 2022. The Philippine Rice Information System (PRiSM): An Operational Monitoring and Information System on Rice . In: Vadrevu, K.P., Le Toan, T., Ray, S.S., Justice, C. (eds) Remote Sensing of Agriculture and Land Cover/Land Use Changes in South and Southeast Asian Countries. Springer, Cham. https://doi.org/10.1007/978-3-030-92365-5_7

Mansaray, L. R., Zhang, D., Zhou, Z., and Huang, J. 2017. Evaluating the potential of temporal Sentinel-1A data for paddy rice discrimination at local scales. Remote Sensing Letters. 8 (10), pp. 967-976.

MWRI. 2005. Water for the future. National Water Resources Plan 2017. Ministry of Water Resources and Irrigation.

Nelson A, Setiyono T, Rala AB, Quicho ED, Raviz JV, Abonete PJ, et al. 2014. Towards an operational SAR-based rice monitoring system in Asia: examples from 13 demonstration sites across Asia in the RIICE project. Remote Sens. 6:10773–10812.

Nguyen, D. B., Gruber, A., and Wagner, W. 2016. Mapping rice extent and cropping scheme in the Mekong Delta using Sentinel-1A data.Remote Sensing Letters. 7 (12), pp. 1209-1218.

Nguyen, T.S., Chen, C., Chen, C.R.,, Toscano, P., Cheng, Y.S., Guo, H.Y., Syu, C. 2021. A phenological object-based approach for rice crop classification using time-series Sentinel-1 Synthetic Aperture Radar (SAR) data in Taiwan. International Journal of Remote Sensing 42:7, pages 2722-2739.

Raviz, J., Laborte, A., Gatti, L., Mabalay, M.R., Holecz, F. 2018. Detection of start of season dates of rice crop using SAR and optical imagery, Central Luzon, Philippines. In Proceedings - 39th Asian Conference on Remote Sensing:

Remote Sensing Enabling Prosperity, ACRS 2018 (Vol. 2, pp. 815-822). Asian Association on Remote Sensing.

Ribbes, F., and Le Toan, T. 1999. Rice field mapping and monitoring with RADARSAT data. International Journal of Remote Sensing. 20 (4), pp. 745-765.

Rosenqvist, A. 1999. Temporal and spatial characteristics of irrigated rice in JERS-1 Lband SAR data. International Journal of Remote Sensing. 20, pp.1567−1587.

Tolba, RA., El-Shirbeny, M.A., Abou-Shleel, SM., El-Mohandes, MH. 2020. Rice Acreage Delineation in the Nile Delta Based on Thermal Signature. Earth Systems and Environment 4, 287–296 (2020). https://doi.org/10.1007/s41748-019-00132-x

Yu, Q., You, L., Wood-Sichra, U., Ru, Y., Joglekar, AKB., Fritz, S., Xiong, W., Lu, M., Wu, W., Yang, P. 2020. A cultivated planet in 2010: Part 2: The global gridded agricultural-production maps. Earth System Science Data, 12, 3545-3572. https://doi.org/10.5194/essd-12-3545-2020